MASS TRANSFER AT THE EXTRACTION FROM POROUS SLABS

Marcela POPA, Eugenia Teodora IACOB TUDOSE, Ioan MAMALIGA*

Department of Chemical Engineering, Faculty of Chemical Engineering and Environmental Protection, "Gheorghe Asachi" Technical University of Iasi, 73 Prof. dr. docent Dimitrie Mangeron Street, Iasi, 700050, Romania

Abstract

The paper presents a study on the mass transfer achieved in the extraction of a high solubility salt in water from a porous inert material in the form of a slab. The obtained experimental data allowed the calculation of the salt mass transfer coefficient when a slab is washed with demineralized water of known flowrate. The driving force of mass transfer is given by the difference between the concentration at the solid-liquid interface and the liquid phase calculated using conductivity measurements.

Key words: mass transfer coefficient, porous slabs, horizontal flow

1. Introduction

There are many applications involving the mass transfer from a solid porous material in the form of a slab to a flowing liquid phase. Thus, unwanted organic or inorganic products can be removed from contaminated soils or electronic materials [1, 3, 4, 11, 17, 18]. Another example is the extraction of residual oil from underground rocks [12, 14], or the extraction of compounds from plant or animal structures, in food or pharmaceutical industries [1, 15, 19, 23].

The diffusion process underlies the mass transfer of the main compound that can be compacted or dispersed in the porous structure. During extraction, the concentration of the dissolved substance varies. The nature of the interactions between the solute and the solid matrix as well as the solid-liquid extraction mechanism, depend on the composition and origin of the solid material, generally less known. In principle, solutes can be adsorbed on the specific surface of the sample particles, in which case the interaction can be overcome using a solvent with high solute affinity, or the molecules can be physically encapsulated in the sample matrix, in which case for extraction the physical destruction of the solid material texture is necessary.

* Corresponding author: E-mail address: imamalig@tuiasi.ro (Ioan Mamaliga).

If the solute is evenly distributed in the solid matrix, the one near the solid surface will be dissolved immediately, leaving behind the porous structure of the solid residue. In this way, the solvent penetration to another level in the solid matrix is facilitated and another amount of solute is dissolved. Progressively, the process becomes more and more difficult and the degree of extraction decreases.

The porous structure geometry of the solid determines its physical and chemical properties, influencing the fluid flow hydrodynamics and the transport of extracted solute.

The process is difficult to control, on one hand, due to the liquid phase flow and on the other hand due to difficulties in estimating the solid-liquid phase contact surface. It is necessary to study this process at the interface of the two phases involved.

There are studies [6, 7] for unidirectional fluid flows through porous solids obeying Darcy's law, where the mass transfer coefficient depends on the liquid solute concentration, the liquid saturation concentration, the solid porosity, the extraction time period, the dispersion coefficient and the Darcy velocity. However, considering the pore interface variability, one can use instead of the Darcy equation, the Brinkman equation [19], or the Darcy equation with a suitable discontinuity limit condition [16].

The experimental results presented in this study were processed to:

- determine the compound extraction rate from a solid matrix;
- determine the global mass transfer coefficient for the compound extraction from the solid matrix;
- study the influence of some types of porous supports on the process.

2. Experimental

The mass transfer study for solid-liquid extraction from slabs was performed using an experimental set-up shown in Figure 1.

In the device (1) the solid sample in the form of a slab was placed. The perspex device (1) is constructed to prevent the liquid phase from moving over the top surface of the slab. The flushing fluid from the constant level feeding tank (2) passes over a threshold placed just before the slab, causing it to be uniformly soaked. The fluid flow rate, measured with a flow meter, is laminar. The salt solution conductivity determined with the conductivity meter (4) is measured at the outlet of the device.

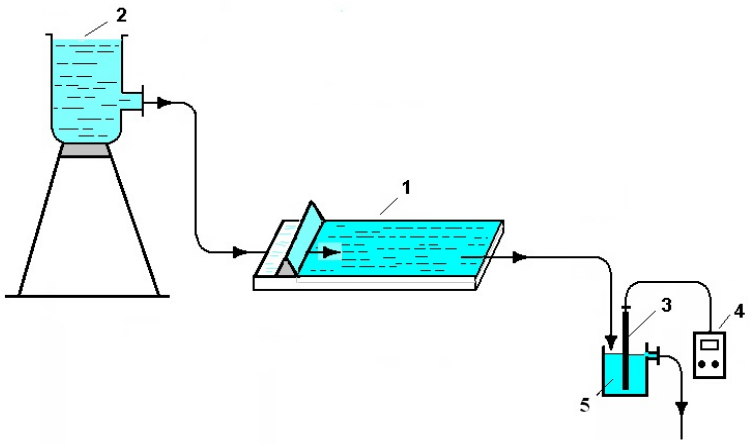

Fig. 1. The schematic diagram of the solid-liquid extraction experimental set-up with slabs; 1-extraction device, 2-vessel solvent, 3-conductivity probe, 4-conductometer, 5-sample cell

Materials and Operating Conditions

In this study, three types of materials with different porosities and therefore, different mass transfer behavior, were used, namely: sandstone, BCA and refractory brick.

In solid-liquid extraction, each porous slab used was solvent-free, polished, washed with water and oven-dried for 6 hours, at 80° C. Subsequently, impregnation was attained by immersion in 5% NaCl solution, for 48 hours. The salt extraction was carried out at 20 ± 1 ° C and atmospheric pressure, using fresh solvent. The washing fluid used was demineralized water at a flow rate of 20 L/h, with a film thickness of 1-2 mm. The extract salt concentration was measured every 60 seconds.

The porous materials used in the solid-liquid extraction were subjected to SEM-EDX analysis and the results are shown in Table 1.

Table 1.

Sample composition in chlorine and sodium, before and after impregnation

Sample/composition	Chlorine (%)	Sodium (%)
Nonimpregnated sandstone	-	0.8122
Impregnated sandstone	1.4107	1.3131
Nonimpregnated Brick	-	0.4522
Impregnated Brick	29.6754	29.4638
Nonimpregnated BCA	-	0.4926
Impregnated BCA	2.0140	3.4970

The salt solution samples obtained after extraction, from the device (1), were conductometrically measured and analyzed, based on a calibration curve experimentally determined, at the working temperature.

3. Results and discussions

The experimental data were processed based on the following hypotheses:
- the salt is evenly distributed in the porous solid material;
- the pore shape and size remain constant;
- the transfer is made over the entire porous slab surface which is completely wetted by the liquid phase;
- the flow is laminar (horizontal liquid film);
- the liquid phase salt concentration is the same, at any point.

The solute flux transferred in liquid phase is given by the equation:

$$N_A = k \cdot A(c_A^* - c_A) \tag{1}$$

The extraction rate is estimated using the following equation:

$$v_e = \frac{\Delta m}{A \cdot \Delta t_i} \tag{2}$$

The extracted component flux can be calculated with:

$$N_A = M_v \cdot \Delta c = M_v \cdot (c_{A_i} - c_{A_0}) \tag{3}$$

Notations

M_v - the liquid flowrate (demineralized water) at the sample layer entrance, m^3/s

Δt_i - time interval between two consecutive readings, s

$c_A^* - c_A$ - the driving force of the mass transfer, kg/m^3

v_e - the extraction rate, Kg/m^3s

k - the global mass transfer coefficient, $m\ s^{-1}$

A - the mass transfer area, m^2

c_A^* - the salt concentration extracted at equillibrium, Kg/m^3

c_{Ai} - the salt concentration extracted at the t_i moment, Kg/m^3

c_{A0} - the salt concentration extracted at the initial moment, Kg/m^3

t - the extraction time, s.

The obtained experimental results are shown in Figure 2 as the extract salt concentration variation with time. One can observe that the maximum concentration value is at the beginning of the process when salt elution takes place on the surface of the solid sample. This maximum value was obtained for all the studied samples. As the liquid phase penetrates the solid material pores and the salt extraction takes place, followed by the salt migration towards the slab and its transfer in the liquid film, the amount of extracted salt decreases. This results in an increase of the extraction time.

3.1. The extraction rate

The extraction rate was calculated as the mass of the extracted salt from the surface area unit, in the time unit, according to the equation (2).

3.1.1. Ceramic sandstone slabs

The studies were carried out on two types of ceramic sandstone slabs, marked sandstone 1 and sandstone 2, of similar dimensions. Figures 3 and 4 show the extraction rate profiles in time, for the two types of sandstone. One can observe an important decrease in the extraction rate in the first 300-400 s, after which the curve slope becomes very small.

The obtained values for the extracted salt flux are very similar for the same type of sample used in the study, either sandstone 1 or sandstone 2, however different values were recorded for the extraction rate values for the two different types of sandstone.

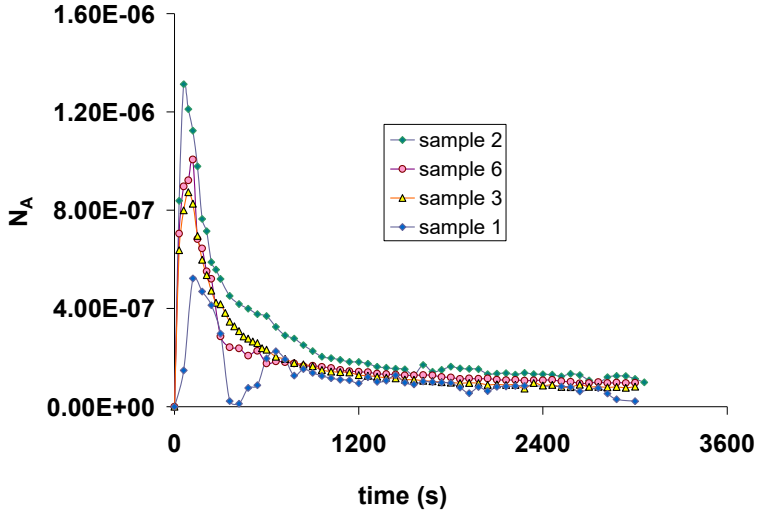

Fig. 2. Variation of the extracted salt flux in time for the sandstone slab 1

The extraction rate has values ranging from $1 \cdot 10^{-5} – 2.6 \cdot 10^{-4}$ Kg / m^2 s. Higher values were recorded for sandstone slabs 2. The analysis of the two graphs from Figures 3 and 4 indicates two stages of the process. In the first stage, the extraction rate records minimum values in the range of $4.01 \cdot 10^{-5}$ - $7.26 \cdot 10^{-5}$ Kg / m^2s, corresponding to the time of 300 s, for the six samples used, when a salt extraction takes place from the slab surface.

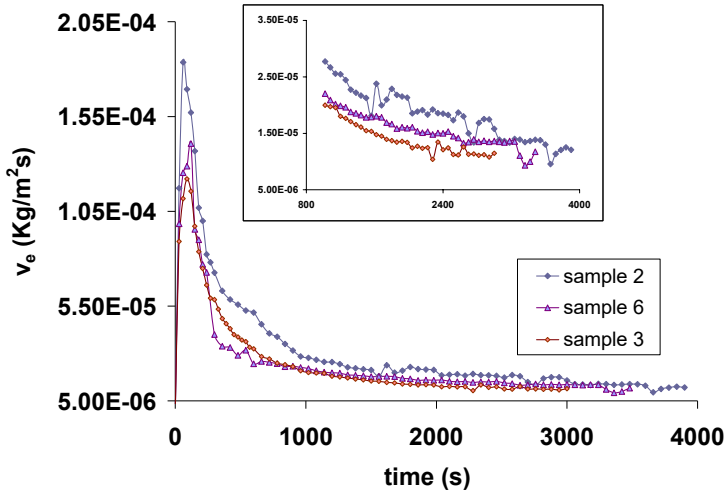

Fig. 3. The extraction rate for sandstone slabs 1

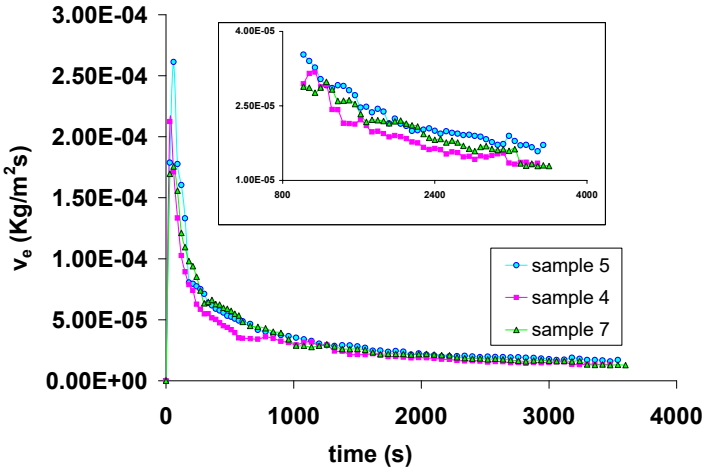

Fig. 4. The extraction rate for sandstone slabs 2

This is followed by a gradual penetration of the washing liquid into the pores both in the horizontal and in the depth directions, according to the model shown in figure 6. This is the decisive stage of the process. Salt extraction takes place slowly due to the slow liquid diffusion into the pores, followed by the salt dissolution and the liquid phase diffusion towards the exterior of the solid slab.

3.1.2. Ceramic brick slabs

The values of the NaCl extraction rate from brick slabs lie within the range of $8 \cdot 10^{-5}$- $2 \cdot 10^{-3}$ Kg / m^2 s, for an extraction time of 3000 s, as seen in Figure 5. For the brick samples, the slope change, corresponding to the passage to the second stage of the extraction, takes place at a time t = 210 s and the rate values obtained are $5.8 \cdot 10^{-4}$-$6.6 \cdot 10^{-4}$ Kg / m^2s.

For the second stage, the extraction rate profile has a much higher slope for brick than for the sandstone slabs. This, as well as the higher extraction rate values, can be explained by a better diffusion determined by the material characteristics.

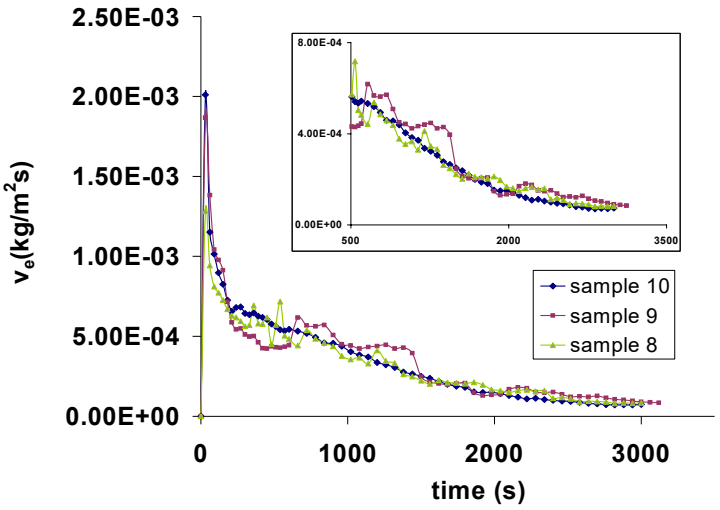

Fig. 5. The extraction rate for brick slabs

3.1.3. BCA ceramic slabs

BCA porosity is superior to brick and sandstone samples. Thus, the values recorded for the salt extraction rate are much higher than those obtained for the sandstone and the brick materials. The maximum obtained rate values are around $4 \cdot 10^{-3}$ Kg / m^2 s and the minimum rate values are approximately $7 \cdot 10^{-5}$ Kg / m^2

s, as shown in Figure 6. The salt extraction behavior reflected by the curve shape for the BCA samples resembles that of the brick samples.

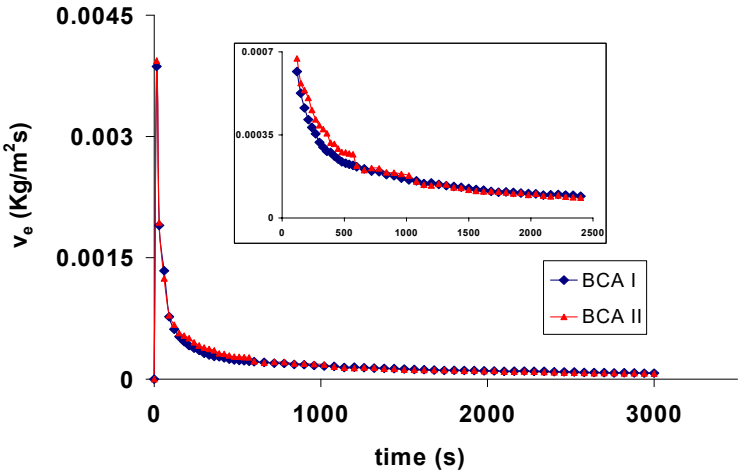

Fig. 6. The extraction rate for BCA slabs

Analyzing, however, the profile given by the extraction rate values, we find that it is close to the one obtained at the extraction from the sandstone samples. It is noted that for the BCA slabs, the slope for the second stage of the process, which begins around 210 s, is small, and the extraction rate values for the two material samples are very close.

3.2. Mass transfer coefficient

According to [21], a 2D model is efficient to study the mass transfer in a slab. According to the two films theory of Lewis, the global mass transfer coefficient is given by the mass transfer coefficient in the continuous liquid phase and the mass transfer coefficient in the solid phase. As a result, we consider that the process takes place according to the model shown in Figure 7, with a laminar liquid phase flow in thin film and the extraction taking place in two stages. In the first step, the salt is washed from the surface of the solid material sample. In the second step, according to the model shown in Figure 7 and the equation (1), the salt extraction from the material pores takes place, followed by the diffusion of the liquid phase towards the upper surface of the solid slab.

In the first stage of the process, the mass transfer coefficient is given by the mass transfer coefficient in the liquid:

$$\text{for } \delta_p = 0 \qquad k \cong k_L \text{ , where } k_L = \frac{D_{salt}}{\delta} \tag{4}$$

In the second stage, at large time values, the extraction coefficient is determined by the mass transfer coefficient in the liquid phase and by the salt effective diffusion coefficient from the solid material in the liquid phase:

for $\delta_p \geq 0$ $\quad k = f(k_L, k_s)$, where $k_s = \dfrac{D_{ef}}{\delta_p}$, thus : $k = f\left(k_L, \dfrac{D_{ef}}{\delta_p}\right)$

or $k = \dfrac{1}{\dfrac{1}{k_L} + \dfrac{\delta_p}{D_{ef}}}$ (5)

where: k is the overal mass transfer coefficient, m·s^{-1}

k_L - mass transfer coefficient in lichid phase, m·s^{-1}

D_{ef} - the effective diffusion coeficient in the solid pores

δ - the liquid film thickness, m

δ_p - the salt diffusion distance towards the surface of the porous solid material, m

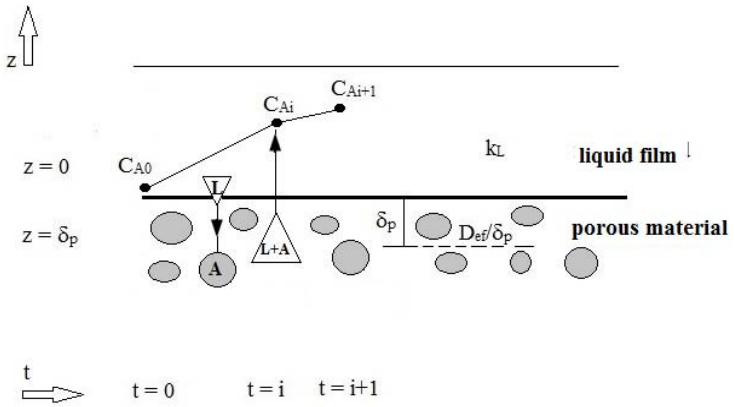

Fig. 7. Salt extraction model from a porous slab

The mean driving force of the mass transfer, Δc_{mean}, decreases with time, on one hand, due to the increase in the salt concentration of the liquid phase, and on the other hand, due to the decrease in the salt concentration of the liquid phase inside the porous matrix. Figure 8 shows the decreasing profile of the salt concentration in the solid matrix in time and the decreasing driving force of the process.

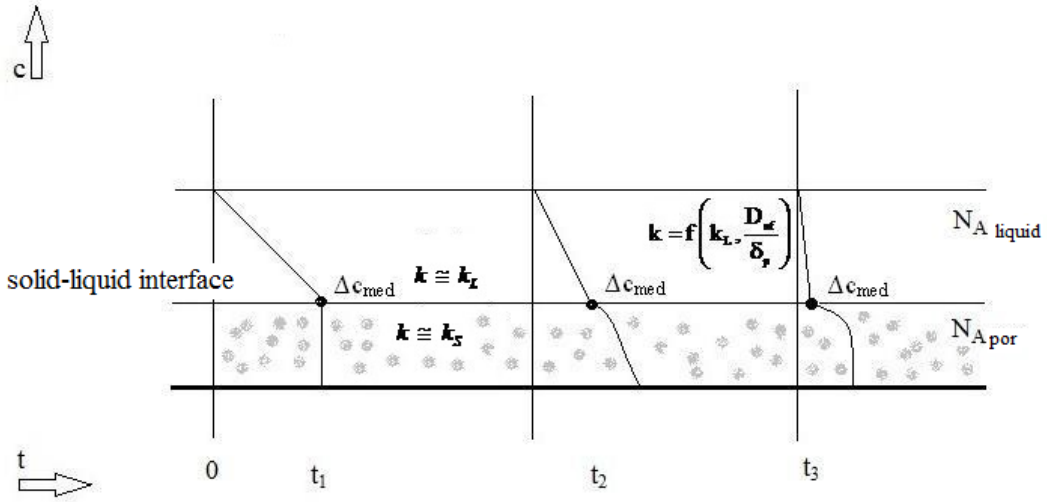

Fig. 8. Concentration profile near the solid-liquid interface

In Equation (5), the term that changes over time is δ_p, since the salt diffusion distance increases as the process unfolds, k_L and D_{ef} having constant values over time. It is the time that determines the process in the second step as the liquid phase diffusion distance into and out of the pores increases.

Based on the equations (1) and (3) and using the obtained experimental results the average mass transfer coefficient was calculated with the following equation:

$$k_L = \frac{N_A}{A \cdot \Delta c_{mean}}, \quad (m/s) \tag{6}$$

The obtained experimental values were compared with the values calculated using existing equations in the literature for laminar flow. Thus, according to [22], for the average mass transfer coefficient from a solid surface with a characteristic length L, under laminar flow conditions, the proposed correlation is:

$$Sh = 0.664 \cdot Re^{0.5} Sc^{0.33} \tag{7}$$

valid for $Re < 3 \times 10^5$ şi $0.6 < Sc < 2500$, where:

$$Sh = \frac{k_L \cdot L}{D_{ef}} \quad \text{is the Sherwood number} \tag{8}$$

$$\mathrm{Re} = \frac{4\Gamma}{\eta} \text{ is the Reynolds number, with } \Gamma = \frac{4M_m}{P} \text{ [9]} \quad (9)$$

$$\mathrm{Sc} = \frac{\eta}{\rho \cdot D_{ef}} \text{ is the Schmidt number} \quad (10)$$

with: M_m - the mass liquid flowrate (Kg/s);
P – the wetted perimeter (m);
η, ρ - the liquid dynamic viscosity and density, respectively;
L- the characteristic length, calculated as the equivalent diameter of the liquid film, $L = \frac{4A}{P}$ (m);
A - flow cross-sectional area of liquid.

3.2.1. Sandstone ceramic slabs

The graphs in Figures 9 and 10 present values obtained by applying the equation (6) to the experimental data regarding the salt extraction from sandstone slabs 1 and 2. Similar to the extraction rate, the graphical representation of mass transfer coefficient has a greater slope for the type 2 sandstone than the type 1, indicating a slower extraction in the latter case.

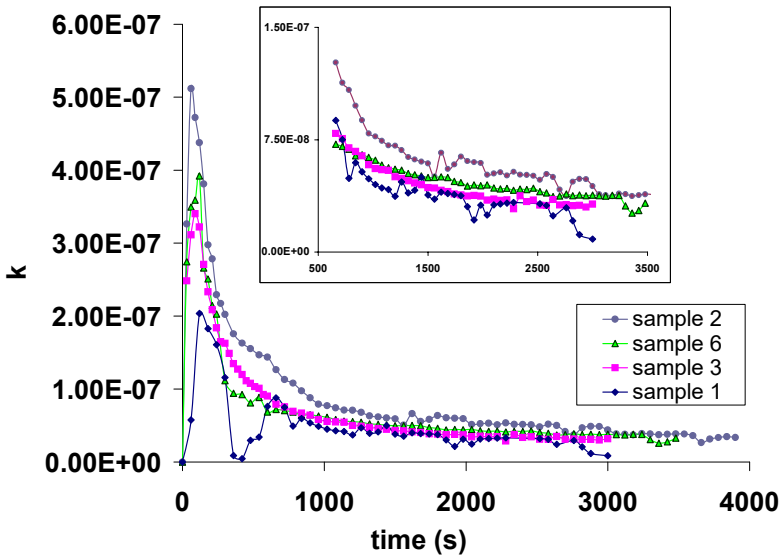

Fig. 9. Mass transfer coefficient for NaCl extraction from sandstone slabs 1

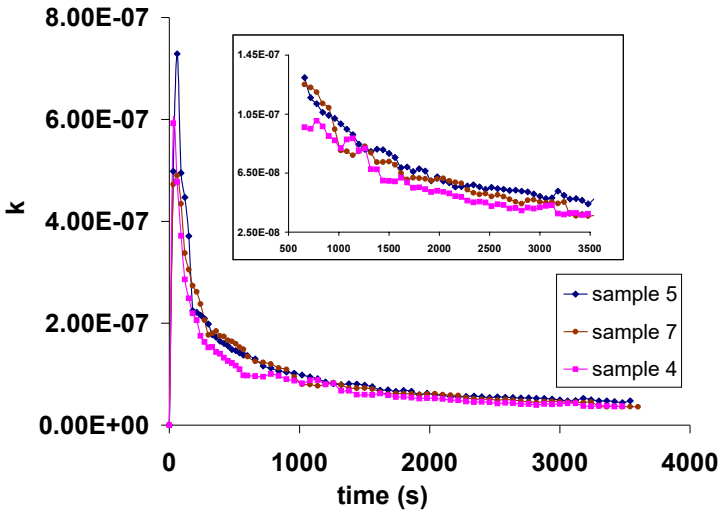

Fig. 10. Mass transfer coefficient for NaCl extraction from sandstone slabs 2

The mass transfer coefficient values for the sandstone slabs are between $7.19 \cdot 10^{-8}$ - $1.29 \cdot 10^{-7}$ Kg / m^2s at 660 s and $8.66 \cdot 10^{-9}$ - $4.93 \cdot 10^{-7}$ Kg / m^2s at 3000 s. The values are closer for the type 2 sandstone samples. It is noted that there is no predictable distribution of these points.

3.2.2. Brick slabs

Similar to the salt extraction from sandstone slabs, in brick samples, the mass transfer coefficient measured values do not fit a particular profile. The maximum values at t = 660 s are in the range of $1.23 \cdot 10^{-6}$ - $1.72 \cdot 10^{-6}$ Kg / m^2s and at t = 3000 s the interval is much narrower $2.04 \cdot 10^{-7}$ - $2.52 \cdot 10^{-7}$ Kg / m^2s, as shown in Figure 11.

3.2.3. BCA slabs

The mass transfer coefficient values obtained for the two brick samples are very close, especially over the time interval 600 s - 3000 s. The maximum values are between $6.02 \cdot 10^{-7}$ Kg / m^2s and $6.15 \cdot 10^{-7}$ Kg / m^2s and the minimum values in the range $1.94 \cdot 10^{-7}$ Kg / m^2s - $2.04 \cdot 10^{-7}$ Kg / m^2s.

Unlike the other types of samples used, for BCA slabs a uniform distribution of the mass transfer coefficient values is observed in Figure 12. The graph has a high slope at the beginning, specific to the first stage of the extraction process, while in the second stage, this becomes much smaller due to the slow extraction process from the solid material pores.

Figure 13 shows a comparison among the mass transfer coefficients variations with time for the three types of studied porous materials. There is a large difference between the values obtained for sandstone and brick slabs.

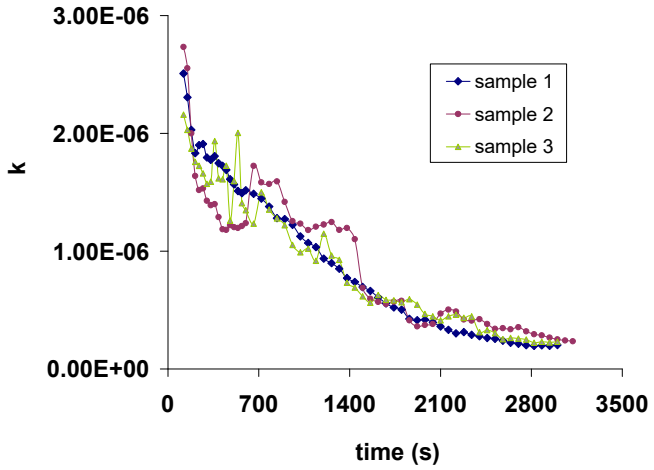

Fig. 11. Mass transfer coefficient for NaCl extraction from brick slabs

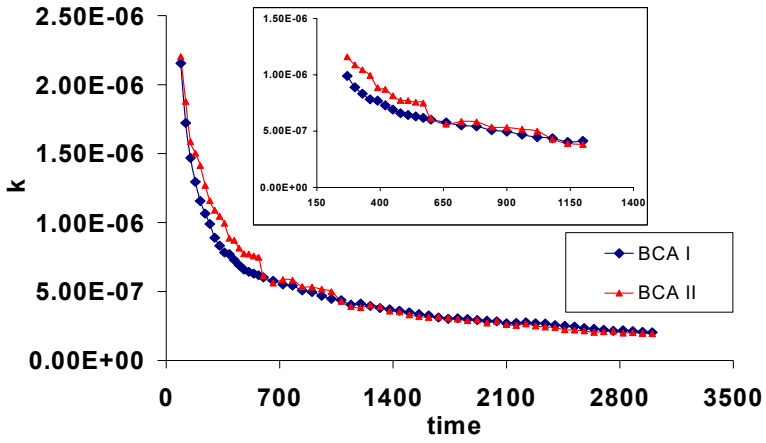

Fig. 12. Mass transfer coefficient for NaCl extraction from BCA slabs

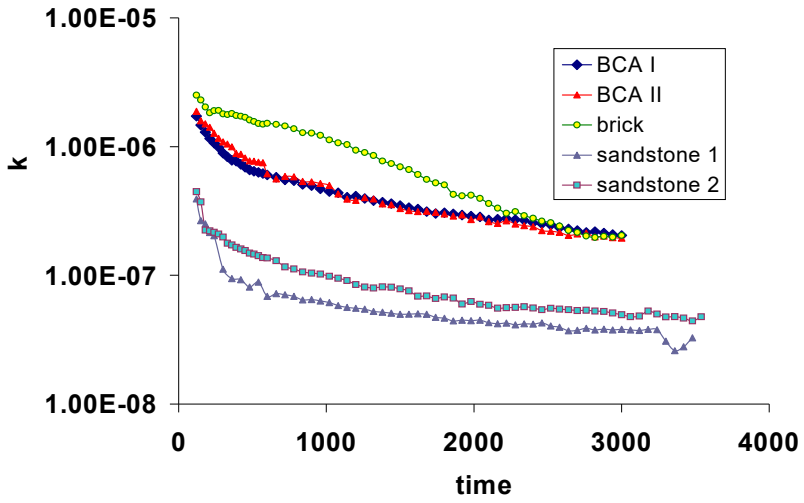

Fig. 13. Comparison of mass transfer coefficients for NaCl extraction from different types of slabs

For the BCA and the brick slabs, the mass transfer coefficient values are very close at times greater than 2000 s, but also, in the first stage of the process, at times shorter than 210 s. The highest slope is observed for the brick samples, which shows that in this case, the largest salt amount is removed up to t = 2000 s. On the other hand, the sandstone and the BCA slopes are smaller than for the brick samples, thus the amounts of extracted salt are smaller, but equal for the two types of BCA samples. The results obtained by applying the equation (7) for the volume flow at the inlet and the outlet of the porous solid slab, subjected to extraction, are shown in Table 2:

Table2:

Comparison between mass transfer coefficients for all types of samples

Slab type	k_L(eq. 7)	$k_{Lexperimental\ I\ (0 - 120\ s)}$	$k_{Lexperimental\ II\ (120 - 3000\ s)}$
sandstone	$1 \cdot 10^{-6}$	$2.04 \cdot 10^{-7} - 4.47 \cdot 10^{-7}$	$8.66 \cdot 10^{-9} - 4.93 \cdot 10^{-7}$
brick	$1.99 \cdot 10^{-6}$	$2.16 \cdot 10^{-6} – 2.73 \cdot 10^{-6}$	$2.04 \cdot 10^{-7} - 2.52 \cdot 10^{-7}$
BCA	$2.11 \cdot 10^{-6}$	$1.72 \cdot 10^{-6} - 1.88 \cdot 10^{-6}$	$1.94 \cdot 10^{-7} - 2.04 \cdot 10^{-7}$

4. Conclusions

The results from this study indicate the following:

- the extraction rate and mass transfer coefficient are influenced by the type of sample used (its structure);

- for both the extraction rate and the mass transfer coefficient, the highest values are obtained for the brick samples and the minimum for the slabs, proportional to the porosity and the amount of salt contained, but also depending on the pore structure network evenness;

- the mass transfer coefficient according to the equation (3) is proportional to the driving force of the process, which decreases over time as the difference between the salt concentration in the liquid and the salt concentration at the surface of the porous solid decreases;

- high values for the mass transfer coefficient are obtained according to the high salt sample concentration. The highest value is recorded for the brick samples, having the highest salt content (according to Table 1);

- the comparison between experimental data and those obtained by applying the equation (7) shows a good agreement for the low-time extraction (domain I), but for time values greater than 120 s, the equation (7) cannot be applied. For this domain (II), the influence of diffusion in the material pores is important.

- the mass transfer coefficient obtained experimentally is a global one and sums up the resistance to mass transfer from the interface to the liquid as well as the diffusion resistance inside the porous material. The coefficient obtained from the calculations is the only one describing the mass transfer in the liquid film.

REFERENCES

[1] Aissou, M., Chemat-Djenni, Z., Yara-Varon, E., Fabiano-Tixier, A-S., Farid, C., Limonene as an agro-chemical building block for the synthesis and extraction of bioactive compounds, *Comptes Rendus Chimie*, 20, (2017), 346-358.

[2] Augustijn, D.C. M., Jessup, R. E., Rao, P.S. C., Wood, A. L., Remediation of contaminated soils by solvent flushing, *Journal of environmental engineering-ASCE*, 120, (1994), 42.

[3] Cabidoche, Y.-M, Achard R., Cattan P., Clermont-Dauphin C., Massat F., Sansoulet J., Long-Long-term pollution by chlordecone of tropical volcanic soils in the French West Indies: A simple leaching model accounts for current residue, *Environmental Pollution*, 157(5), (2009), 1697–1705.

[4] Cuenot F., Meyer M., Bucaille A., Guilard R., A molecular approach to remove lead from drinking water, *Journal of Molecular Liquids*, 118, (2005), 89– 99.

[5] Dalgren K.E., Düker A, Arwidsson Z, von Kronhelm T, van Hees P.A., Re-cycling of remediated soil – Evaluation of leaching tests as tools for characterization, *Waste Management*, 31, (2011), 215–224.

[6] Halder, A., Datta, A. K., Surface heat and mass transfer coefficients for multiphase porous media transport models with rapid evaporation, *Food and Bioproducts Processing*, 90, Issue 3, (2012), 475–490.

[7] Krenn, J., Baesch, S., Schmidt-Hansberg, B., Baunach, M., Scharfer, P., Schabel, W.,Numerical investigation of the local mass transfer on flat plates in laminar flow, *Chemical Engineering and Processing,* 50, (2011), 503–508.

[8] Librán, C.M., Mayor, L, Garcia-Castello, E.M., Vidal-Brotons, D., Polyphenol extraction from grape wastes: Solvent and pH effect, *Agricultural Sciences*, 4, (2013), 56-62.

[9] Tudose, R.Z., Mămăligă. I., Coeficienţi individuali de transfer de masă la curgerea lichidelor în filme subţiri, *Revista de Chimie*, 45, (1994), 652-662.
[10] Nayak, C.A., Chethana, S., Rastogi, N.K., Raghavarao, K.S.M.S., Enhanced mass transfer during solid–liquid extraction of gamma-irradiated red beetroot, *Radiation Physics and Chemistry*, 75, (2006), 173–178.
[11] Park, Y.S., Moon, J.H., Kim, D.S., Ahn, K.H., Treatment of a polluted stream by a fixed-bed biofilm reactor with sludge discharger and backwashing system, *Chemical Engineering Journal,* 99, (2004), 265–271.
[12] Pathak, S., Singh, T., A mathematical modelling of imbibition phenomenon in inclined homogenous porous media during oil recovery process, *Perspectives in Science*, 8, (2016), 183-186.
[13] Pinho, G. P. de., Neves, A. A., Queiroz, M. E. L. R. de., Silvério, F. O., Pesticide determination in tomatoes by solid–liquid extraction with purification at low temperature and gas chromatography, *Food Chemistry*, 121, (2010), 251–256.
[14] Salehi, M.M., Omidvar, P., Naeimi, F., Salinity of injection water and its impact on oil recovery absolute permeability, residual oil saturation, interfacial tension and capillary pressure, *Egyptian Journal of Petroleum*, 26, (2017), 301-312.
[15] Seikova I., Simeonov E., Ivanova E., Protein leaching from tomato seed - experimental kinetics and prediction of effective diffusivity, *Journal of Food Engineering,* 61, (2004), 165-171.
[16] Tio, K. K., Sadhal, S.S., Boundary conditions for Stokes flows near a porous membrane, *Appl. Sci. Res*., 52, (1994), 1-20.
[17] Tiruta-Barna L., Fantozzi-Merle C., de Brauer C., Barna, R., Leaching behaviour of low level organic pollutants contained in cement-based materials, *Journal of Hazardous Materials B*, 138, (2006), 331–342.
[18] Tsang, C-F., Neretnieks, I, Tsang, Y., Hydrologic issues associated with nuclear waste repositories, *Water Resources Research*, 51, (2015), 6923–6972.
[19] Vafai, K., Thiyagaraja, R., Analysis of flow and heat transfer at the interface region of a porous medium, *International Journal of Heat and Mass Transfer*, 30(7), (1987), 1391-1405.
[20] Vázquez G., Fernández-Agulló A., Gómez-Castro C., Freire M.S., Antorrena G., González-Álvarez J., Response surface optimization of antioxidants extraction from chestnut (*Castanea sativa*), *Industrial Crops and Products,* 35, (2012), 126– 134.
[21] Zeng, Y., Lee, T.-S., Yu, P., Low, H.-T., Numerical study of mass transfer coefficient in a 3D flat-plate, rectangular microchannel bioreactor*, International Communications in Heat and Mass Transfer,* 34, (2007), 217–224.
[22] Welty, R.J., Wicks, C.E., Wilson, R.E., Rorrer, G.L., *Fundamentals of Momentum, Heat, and Mass Transfer*, 5th Edition, John Wiley & Sons, 2008.
[23] Simeonov, E., Koleva, V., Solid-liquid Extraction of Tannins from Geranium Sanguineum L. –Experimental Kinetics and Modelling, *Chemical and Biochemical Engineering Quarterly,* 26(3), (2012), 249–255.